

SOME ELEVATED TEMPERATURE TENSILE AND STRAIN-CONTROLLED FATIGUE
PROPERTIES FOR A 9%Cr1%Mo STEEL HEAT TREATED TO
SIMULATE THICK SECTION MATERIAL

S J Sanderson and S Jacques

United Kingdom Atomic Energy Authority, Risley Nuclear Power
Development Laboratories, Risley, Warrington, England.

ABSTRACT

Current interest has been expressed in the usage of thick section 9%Cr 1%Mo steel, particularly for UK Commercial Demonstration Fast Reactor (CDFR) steam generator tubeplates. This paper presents the results of some preliminary mechanical property test work on a single cast of the steel, heat treated to simulate heavy ruling sections encompassing thicknesses likely to be met in the CDFR context. The microstructures of the simulated thick section material were found to remain predominantly as tempered martensite even at the slowest transformation cooling rates used (50°C/h). The effect of microstructure is reflected in the elevated temperature proof stress, tensile strength and strain-controlled fatigue endurance which were found to be comparable with the properties established for thin section normalised and tempered 9%Cr1%Mo steel. These results are extremely encouraging and, taken in conjunction with the results from other simulation work on this material, further demonstrate the potential of thick section 9%Cr1%Mo steel.

1. INTRODUCTION

Preliminary stress analysis for the CDFR (1981) design has shown that the properties expected of 9%Cr1%Mo steel can be used to advantage over those afforded by 2½%Cr1%Mo steel in the heavy section tubeplate and closure head components of the steam generator unit (SGU). Since the steam tube material has been defined as 9%Cr1%Mo steel(1), the SGUs now present a single major structural material concept with components ranging in section thickness from a few millimetres for the steam tube, to several hundred millimetres for the tubeplate.

Although the mechanical properties of wrought normalised and tempered 9%Cr1%Mo steel have been reliably established for sizes below ca 31mm dia(2, 3), little, if any, data or experience are available on this steel at sections beyond ca 155mm(4). It has therefore been appropriate to mount preliminary tensile property and microstructural studies using available bar stock material heat treated to simulate the thermal history expected for the CDFR SGU tubeplates. These preliminary studies have been fully reported(5) and found to be sufficiently encouraging to provide confidence for the development of the material in thick section. A programme for this development is intended, and further simulation work on heat treated bar stock is being undertaken in the interim before actual forging material becomes available in order to provide comparative data, particularly for fatigue and creep-fatigue testing modes. The present paper gives metallographic, tensile and continuous cycling strain-controlled fatigue data from this interim work programme.

2. EXPERIMENTAL DETAIL

The material used throughout this work was taken from a single cast of 9%Cr1%Mo steel accessible as 31mm dia bar stock for which previously reported elevated temperature tensile and strain-controlled fatigue data are available in the as-received normalised and tempered condition(3). The chemical composition and as-received heat treatment for this material are indicated in Table 1.

The as-received bar was cut to the specimen lengths and heat treated to simulate thermal histories which may occur in heavy section components. These heat treatments are also detailed in Table 1 where it can be seen that two transformation cooling rates have been used, namely 100 and 50°C/h, intended to approximate to air-cooled bar sections at 500 and 1000mm respectively, according to published indicative continuous cooling transformation data available for 9%Cr1%Mo steel(6). All heat treatments were performed in a furnace equipped with solid-state linear-programmable temperature control; thermocouples attached directly to the specimen blanks enabled the temperature to be independently monitored and control was found to be within $\pm 5^{\circ}\text{C}$. After the required heat treatments, the blanks were machined to the final specimen geometries (9mm dia, 5.65 \sqrt{A} gauge length tensile specimens; 7.4mm dia, 12.7mm gauge length fatigue specimens) thereby removing the decarburised/oxidised surface layer formed as a consequence of the heat treatment atmosphere (air). The specimens were finish-machined using cutting depths less than 0.06mm per revolution with soluble oil coolant in order to preserve the microstructural condition and arrive at a final surface finish of better than 20 CLA (ie: an average surface roughness of better than 0.5 μm).

The tensile tests were performed in accordance with BS18 or BS3688 at room and elevated temperature respectively to give the 0.2% proof stress, ultimate tensile strength, % elongation and reduction of area at failure. Vickers indentation hardnesses were taken to BS427 at room temperature from undeformed specimen heads using a 30Kg load and basic metallography conducted on prepared sections to reveal the bulk microstructures. The strain-controlled fatigue tests were performed using a single, dedicated servo-hydraulic testing frame. Particular attention has been given to specimen axiality in the testing machine both during setting-up and throughout the tests; axiality was better than $\pm 25\mu\text{m}$. Fully-reversed axial strain controlled push-pull fatigue tests were conducted in air at a temperature of $525 \pm 2^{\circ}\text{C}$ using a triangular strain waveform at a fixed strain rate of $6.67 \times 10^{-4}/\text{s}$, each test being started in a tension-going ramp. The data were analysed for each continuous cycling test to give the number of cycles to failure (N_f); the measured total strain range; the plastic strain range at ca $N_f/2$; the stress range at $N_f/2$; and the maximum stress range encountered during the test.

3. RESULTS

3.1 Metallographic, Hardness and Tensile Properties

The microstructures for the steel in the as-received and simulated thick section heat treated conditions are all similar and, in both the as-received normalised and tempered condition and the simulative thick section material using 100°C/h as the transformation cooling rate, are wholly tempered martensite with average bulk hardnesses recorded as 213 and 207VPN, respectively. For simulative thick section heat treatments using 50°C/h

as the transformation cooling rate, the microstructural survey indicated an occasional presence of pro-eutectoid ferrite (totalling probably not more than 2 Vol-%) in addition to the tempered martensite matrix; the bulk hardness was recorded as 208 VPN.

The observed similarities in microstructure and hardness for the various heat treatments studied indicate that large differences in the elevated temperature properties are unlikely, and this proved to be the case as can be seen from the tensile properties recorded in Figs 1 and 2. The data given here allow direct comparison between average and 95% confidence limit values for thin section normalised and tempered 9%Cr1%Mo steel derived from a number of different casts(7), actual values for the steel used in the as-received normalised and tempered condition and values obtained from the two simulative thick section heat treatments. These latter heat treatments are seen to give a maximum reduction in 0.2% PS with respect to the available as-received values of ca 15%, with a corresponding maximum reduction in UTS of ca 10%; the strength values do not fall below the lower bounds derived for thin section normalised and tempered material. Comparative failure ductility values are illustrated in Figs 3 and 4 showing a more marked sensitivity to the simulative thick section heat treatments in that the slowest transformation cooling rate appears to be the least ductile although, with the exception of one marginally low R of A value, the ductilities fall within the established 95% confidence limits for thin section normalised and tempered material.

3.2 Strain-Controlled Fatigue Behaviour

Analysed results from the strain-controlled fatigue tests are given in Table 2 and consideration of the stresses sustained at particular total strain ranges shows the softening trend between the as-received and simulated thick section heat treatment conditions which was expected from the monotonic proof and tensile strength behaviour noted previously. When the stresses generated throughout the fatigue tests were analysed in terms of the normalised cycles to failure (N/N_f), the stress response for each heat treatment category was found to be one of cyclic softening up to ca $0.1N/N_f$, a plateau stress level then being established to ca $0.85N/N_f$ with, thereafter, a fairly sharp stress decrease accompanying failure. Low power optical examination of all the fatigue fracture surfaces revealed a topography typical of the transgranular fatigue crack propagation mode and this mode was confirmed on metallographically prepared sections of fractured specimens both for principal and secondary fatigue cracks.

The tabulated results are plotted in logarithmic terms of total strain range vs. cycles to failure in Fig 5, the data exhibiting the expected smooth trend of increasing endurance with decreasing applied strain (and consequently stress) range. Figure 5 also carries data previously generated from the same cast of steel in the as-received normalised and tempered condition with the superimposed average line for continuous cycling strain-controlled fatigue at temperatures not exceeding 525°C (7); it can be seen that all the present data lie above, but close to, the average line. Whilst the data differences are not dramatic in terms of fatigue scatter, representing at most an increase in endurance for material in the as-received condition by a factor of two, they could result from differences in experimentation viz: indirect shoulder extensometry for the earlier data compared with direct gauge length extensometry in the present case. Nevertheless, the important point to note in the comparison is that the data representing continuous cycling strain-controlled fatigue of simulated thick section heat treated material do not transgress the assessed average curve for this property.

4. DISCUSSION

The constitution, transformation and tempering behaviour of the 9%Cr 1%Mo class of steel are well understood(5,8,9) and only the outline principles will be discussed here. The constitution is determined by the relative content of ferrite- and austenite-stabilising elements which may be expressed in terms of a net chromium equivalent. One such expression with composition in wt-% is given(10) as

$$\begin{aligned} \text{Net Cr Equivalent} = & (\% \text{ Cr}) + 6(\% \text{ Si}) + 4(\% \text{ Mo}) + 1.5(\% \text{ W}) + 6(\% \text{ V}) \\ & + 5(\% \text{ Nb}) + 12(\% \text{ Al soluble}) + 8(\% \text{ Ti}) - 40(\% \text{ C}) \\ & - 2(\% \text{ Mn}) - 4(\% \text{ Ni}) - 2(\% \text{ Co}) - 30(\% \text{ N}) - (\% \text{ Cu}) \end{aligned}$$

and illustrates the potent effect of Si, Mo and C in fixing the stable phase fields for plain 9%CrMo steels. Note that although N also has a large coefficient, its absolute concentration level is usually an order of magnitude lower than C, therefore resulting in only a small effect.

When plain 9%Cr1%Mo steels are cooled from the single austenite phase field, the consequent continuous cooling transformation diagram exhibits a wide range of cooling rates which enable transformation of the austenite to martensite(6). Cooling rates slower than a critical value will result in the appearance of pro-eutectoid ferrite in the microstructure, the critical value depending on the net chromium equivalent so that the higher the chromium equivalent, the faster the cooling rate before ferrite formation. The particular effect of silicon has been identified in previous work(5) such that steels with 0.58 or 0.85% silicon content could be cooled in equivalent sections up to ca 1100 and 500mm dia respectively, without forming pro-eutectoid ferrite. It will be noted that the silicon content in the present steel is 0.66% and therefore would be expected to yield an equivalent critical cooling rate for sections intermediate between the previous sizes and this appears to be the case with the presence of small amounts of pro-eutectoid ferrite for the slowest transformation cooling rate used (50°C/h). The austenite-transformed microstructures for 9%Cr1%Mo steel to large equivalent ruling sections are thus seen to remain predominantly martensitic. This behaviour contrasts with that of 2¼%Cr1%Mo steel, a structural material widely used in the power industry, which shows a greater sensitivity to cooling rate and hence section size(11). Thus a simplified comparison of as-transformed microstructures and hardnesses for these two steels presented as a function of approximate equivalent section size takes the appearance of Fig 6; the ability of 9%Cr1%Mo steel to maintain its as-transformed hardness (ie strength) is apparent.

The similarity in microstructure for the various heat treatments of 9%Cr1%Mo steel used in the present work is maintained on subsequent tempering when a complex series of microstructural changes occur, principally the precipitation of alloy carbides from the metastable matrix and a reduction and redistribution of the dislocation component tending towards microstructural stability. The detail of these processes has been described for 9%Cr1%Mo steel(9) and it is sufficient here to note that the similar post-temper microstructures for the simulated thick section heat treated material give comparable elevated temperature tensile and strain-controlled fatigue properties. Closer comparison of the microstructures between the as-received and simulated thick section conditions reveals a tendency towards coarsening in the latter, both in terms of prior austenite grain size and carbide precipitate, as a consequence of the extended austenitising and tempering conditions. This increase in coarseness is

responsible for the comparative softening noted previously for the simulative heat treatments with respect to the as-received condition and may be a contributory factor in the decrease of fracture ductility associated with the slowest transformation cooling rate, although strain-controlled fatigue is less sensitive to these relatively slight microstructural differences.

In general, previous investigations(5,12) using heat treatments to simulate thick section behaviour for 9%Cr1%Mo steel support the present findings in respect of the material's tolerance to a wide range of transformation cooling rates. However, the results obtained from this type of approach should be viewed as indicative only, since other material aspects are not addressed which may be expected in actual thick section components. Thus microsegregation will be influenced by working route and would be expected to differ between product forms. Similarly, chromium equivalent, soak time and cooling rate from the austenitising temperature will influence grain size and pro-eutectoid ferrite formation in a heavy forging such that its surface would experience a longer solution treatment with more rapid effective quench than would be the case at its centre. Furthermore, it should also be recognised that the inter-relationships between cooling rate and section thicknesses used for simulative work are approximate and not absolute. It is believed, however, that a transformation cooling rate of 50°C/h will encompass the heaviest 9%Cr1%Mo steel section contemplated for CDFR and will be used for further simulative work to generate creep-fatigue data in the interim before actual development programme forging material becomes available.

5. CONCLUSIONS

This paper has presented some elevated temperature tensile and strain-controlled fatigue data obtained from a particular cast of 9%Cr1%Mo steel heat treated to simulate thick section material. The principal conclusions are:-

- (i) Microstructures remained predominantly as tempered martensite even for the slowest transformation cooling rate used (50°C/h).
- (ii) The simulative thick section heat treatments produced a decrease in 0.2% PS with respect to the as-received normalised and tempered thin section values of ca 15% with corresponding maximum reduction in UTS of ca 10%.
- (iii) Strength values (both 0.2% PS and UTS) do not fall below the lower bounds derived for thin section normalised and tempered material.
- (iv) The stress response under fatigue conditions for each heat treatment category was observed to be one of cyclic softening up to ca $0.1N/N_f$, a plateau level then being established to ca $0.85N/N_f$ with, thereafter, a fairly sharp decrease accompanying failure.
- (v) Fatigue failure proceeded by transgranular crack propagation in all cases.
- (vi) The strain-controlled fatigue data at 525°C in terms of total strain range and cycles to failure all fall close to (but with slightly higher endurance) the average line for thin section normalised and tempered material.

- (vii) The basic physical metallurgy of the steel is well understood and used to rationalise the observed mechanical behaviour.
- (viii) Overall, these results are extremely encouraging and, taken in conjunction with the results from other simulation work on this class of material, further demonstrate the potential of thick section 9%Cr1%Mo steel.

6. ACKNOWLEDGEMENT

The authors wish to record their appreciation of the experimental work contributed by Mr S R Hindley, Student Assistant, Aston University, Birmingham, as part of this interim programme.

7. REFERENCES

1. HOLMES J A G. Development in UK commercial fast reactor design. Nuclear Energy, Vol 20, 1981, p23, see also Discussion ibid, Vol 21, 1982, p223.
2. ISO 2604/II - TS38. Steel products for pressure purposes - Quality requirements - Part II: Wrought seamless tubes.
3. WOOD D S et al. Mechanical properties data on 9%Cr steel, in Ferritic Steels for Fast Reactor Steam Generators, BNES, London, 1978, p189.
4. NISBETT E G. The production and properties of heavy walled forged vessel shells in 9%Cr1%Mo alloy steel. Paper given at ASM International Conference on Production, Fabrication, Properties and Application of Ferritic Steels for High Temperature Applications, October 1981.
5. ORR J and SANDERSON S J. An examination of the potential for 9%Cr1%Mo steel as thick section tubeplates in fast reactors. Paper given at AIME Topical Conference on Ferritic Alloys for Use in Nuclear Energy Technologies, June 1983.
6. ATKINS M. Atlas of continuous cooling transformation diagrams for engineering steels. British Steel Corporation, 1978.
7. WOOD D S. Materials data for high temperature design. Paper given at I.Mech.E Conference on Experience of Structural Validation in the Nuclear Industry with Emphasis on High Temperature Design, London, 1979.
8. SANDERSON S J. Mechanical properties and metallurgy of 9%Cr1%Mo steel, as for Ref 4.
9. SANDERSON S J. Inter-relationships between mechanical properties and microstructure in a 9%Cr1%Mo steel, as for Ref 3, p120.
10. PATRIARCA P, HARKNESS S D, DUKE J M and COOPER L R. US advanced materials development program for steam generators. Nuclear Technology, Vol 28, 1976, p516.
11. SANDERSON S J. Materials characterisation and tensile properties of 2½%Cr1%Mo steel. RNL Unpublished Work, 1981.

12. MAKIOKA M, KHONO M and SHIBATA T. 5Cr 0.5Mo and 9Cr1Mo heavy steel forgings for pressure vessels. Journal of the Japan High Pressure Institute, Vol 18, 1980, p32.

TABLE 1 : 9%Cr1%Mo STEEL DETAILS

(Bar Stock, 31mm dia)

(i) Chemical Composition

Element	C	Si	Mn	P	S	Cr	Mo	Ni	Al	Cu	Sn	Co
Wt-%	0.10	0.66	0.50	0.013	0.008	8.85	0.95	0.21	0.009	0.15	0.02	0.022

(ii) As-Received Heat Treatment

Normalised after ½h at 950°C, tempered ½h at 750°C.

(iii) Simulative Thick Section Heat Treatments

	Heating Rate to Austenitising Temperature	Austenitise	Cooling Rate to Ambient	Heating Rate to Tempering Temperature	Temper	Cooling Rate to Ambient
(1)	30°C/h	16h at 980°C	100°C/h	30°C/h	2h at 770°C	100°C/h
(2)	30°C/h	16h at 980°C	50°C/h	30°C/h	2h at 770°C	100°C/h

(1) Simulative of ca 500mm section.

(2) Simulative of ca 1000mm section.

TABLE 2 : CONTINUOUS CYCLING STRAIN-CONTROLLED FATIGUE TEST DATA

Test Temperature : 525^oC
 Environment : Air
 Strain Rate : 6.67 x 10⁻⁴/s
 Strain Waveform : Triangular, fully reversed
 Definition of Failure : Complete rupture

Specimen Identity	Measured Total Strain Range %	Plastic Strain Range at N _f /2 %	Stress Range N/mm ²		Cycles to Failure N _f
			Max	N _f /2	
<u>(1) As-Received, Normalised and Tempered (RNL Code 35)</u>					
EW1	1.0	-	+352 -307	+295 -257	2108
EW17	0.72	0.4	+322 -327	+253 -288	3550
EW7	0.51	0.2	+310 -265	+246 -246	8239
EW19	0.42	0.14	+292 -286	+240 -252	20760
<u>(2) Simulative Thick Section Heat Treatment with Transformation Cooling</u>					
Rate at 100 ^o C/h					
FV3	1.0	-	+337 -352	+283 -290	1861
FV6	0.72	0.4	+327 -335	+278 -281	3522
FV5	0.51	0.21	+297 -274	+249 -235	11394
FV4	0.4	0.12	+276 -279	+228 -241	65440
<u>(3) Simulative Thick Section Heat Treatment with Transformation Cooling</u>					
Rate at 50 ^o C/h					
FV9	1.01	0.7	+341 -315	+285 -258	1620
FV10	0.71	0.42	+306 -325	+258 -277	3360
FV11	0.52	0.23	+289 -308	+232 -256	12720
FV12	0.42	0.14	+267 -288	+230 -250	13730

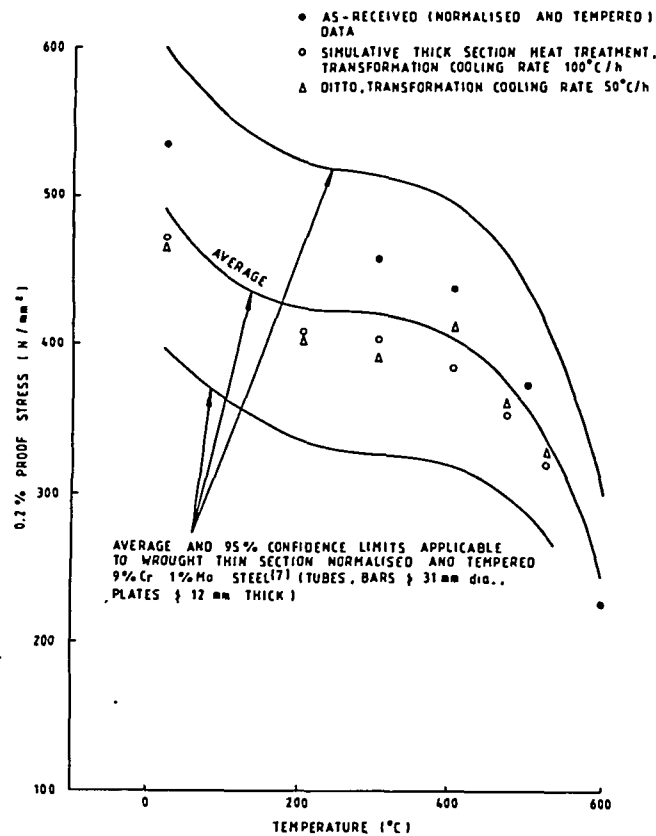


FIG.1 COMPARISON OF 0.2% PROOF STRESS DATA FOR VARIOUS HEAT TREATMENTS OF 9% Cr 1% Mo STEEL

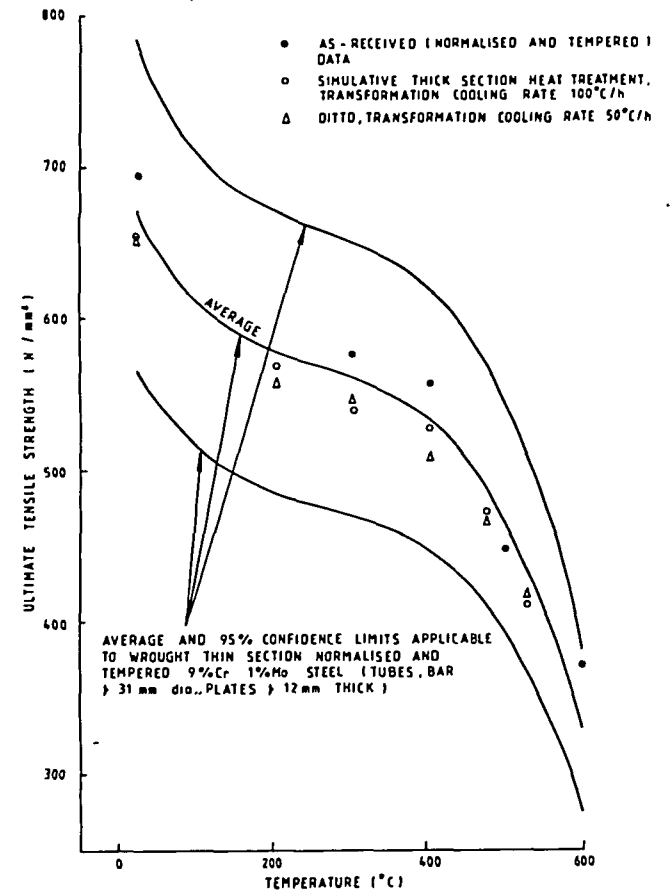


FIG.2 COMPARISON OF TENSILE STRENGTH DATA FOR VARIOUS HEAT TREATMENTS OF 9% Cr 1% Mo STEEL

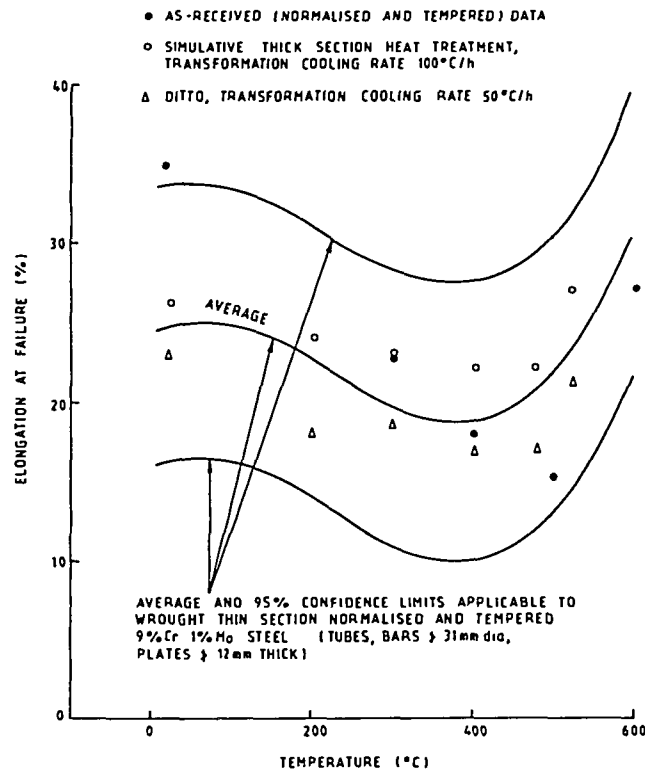


FIG. 3 COMPARISON OF TENSILE ELONGATION DATA FOR VARIOUS HEAT TREATMENTS OF 9%Cr 1%Mo STEEL

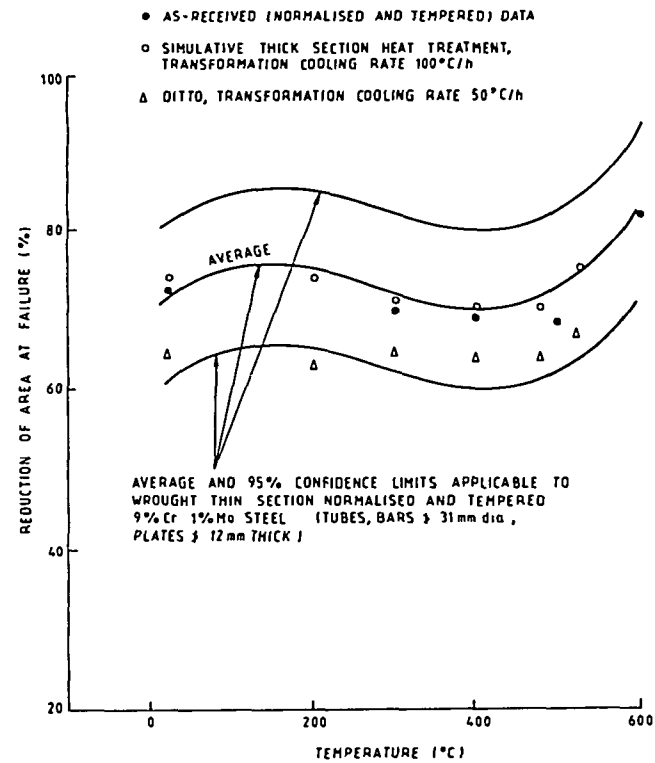


FIG. 4 COMPARISON OF TENSILE REDUCTION OF AREA DATA FOR VARIOUS HEAT TREATMENTS OF 9%Cr 1%Mo STEEL

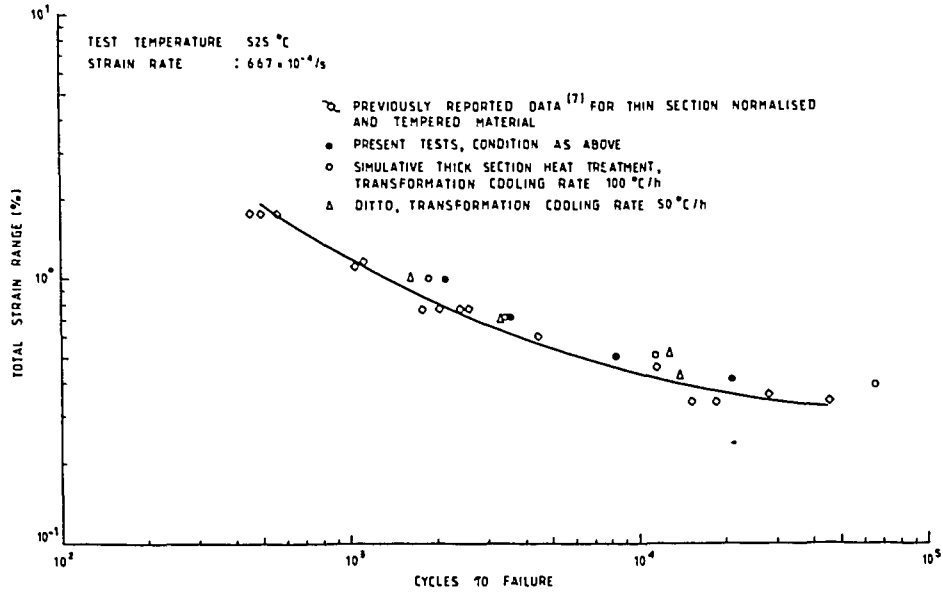


FIG. 5 COMPARISON OF STRAIN-CONTROLLED CONTINUOUS CYCLING FATIGUE DATA FOR VARIOUS HEAT TREATMENTS OF 9% Cr 1% Mo STEEL

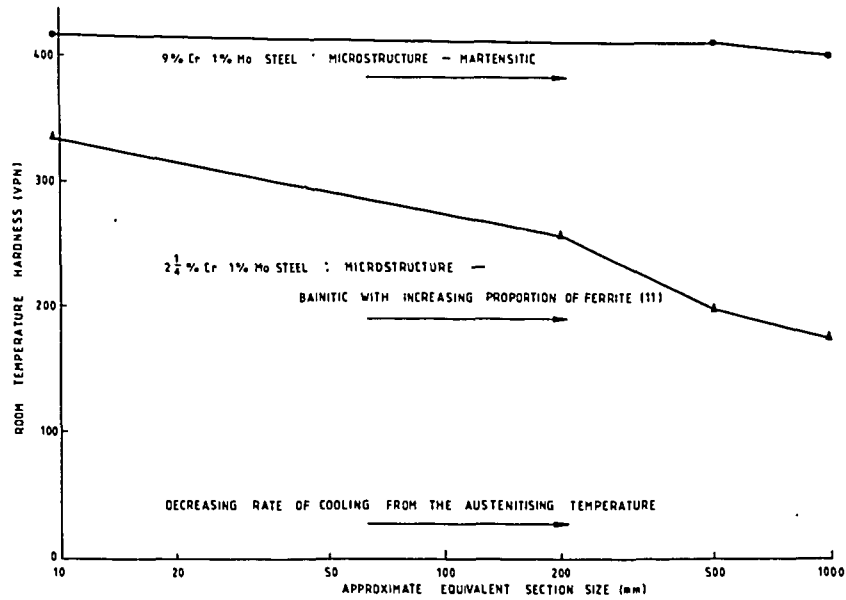


FIG. 6 COMPARATIVE HARDNESS VALUES FOR 9% Cr 1% Mo AND 2 1/2% Cr 1% Mo STEELS IN THE AS-COOLED (UNTEMPERED) CONDITION WITH RESPECT TO SIMULATED SECTION SIZE